Epitaxial $La_{0.67}Sr_{0.33}MnO_3/La_{0.67}Ba_{0.33}MnO_3$ superlattices

Land J. Belenky
Department of Materials Science and Engineering, University of Wisconsin, 1550 Engineering Dr-2165 ECB, Madison, Wisconsin 53706

Xianglin Ke
Department of Physics, University of Wisconsin, 301B Sterling Hall–475 N. Charter St., Madison, Wisconsin 53706

Mark Rzchowski
Department of Physics, University of Wisconsin, 301B Sterling Hal–475 N. Charter St., Madison, Wisconsin 53706

C. B. Eom[a)]
Department of Materials Science and Engineering, University of Wisconsin, 1550 Engineering Dr-2165 ECD, Madison, Wisconsin 53706 and Department of Physics, University of Wisconsin, Madison, Wisconsin 53706

(Presented on 9 November 2004; published online 11 May 2005)

Artificially layered superlattices allows manipulation of strain and the study of dimensional crossover by introducing additional degrees of freedom not found in bulk materials. Superlattices of the colossal magnetoresistive materials, $La_{0.67}Sr_{0.33}MnO_3$ (LSMO) and $La_{0.67}Ba_{0.33}MnO_3$ (LBMO) have been grown by pulsed laser deposition with high-pressure *in situ* reflection high-energy electron diffraction on (001) $SrTiO_3$ substrates. X-ray diffraction shows several sets of superlattice peaks indicating 90 Å periodicity. A high T_c for the LSMO and independent switching of LSMO and LBMO at low temperatures is found. © *2005 American Institute of Physics*.
[DOI: 10.1063/1.1850384]

Colossal magnetoresistive (CMR) materials have been the subject of intense research due to their interesting and potentially useful magnetic characteristics. $La_{0.67}Sr_{0.33}MnO_3$ (LSMO)[1] has been the most widely studied due to its high Curie temperature, 340 K. Because of its lattice parameter of 3.871 Å, a natural choice for substrate would be $(LaAlO_3)_{0.3}(SrAl_{0.5}Ta_{0.5}O_3)_{0.7}$, which is cubic and has a lattice parameter of 3.868 Å.[2] However, $SrTiO_3$ (STO) is more attractive because single-terminated, atomically flat surfaces can easily be made.[3,4] The relatively large lattice mismatch between STO and LSMO causes in-plane strain in epitaxial films. This strain is an important parameter contributing to magnetic properties such as Curie temperature, coercivity, saturation magnetization, and anisotropy.[5–7] However, lattice mismatch is also detrimental to crystalline properties, resulting in the formation of a defect region. Wiedenhorst *et al.* observed in cross-sectional transmission electron microscopy that LSMO films grown on STO are fully strained near the interface, have a defect region about 600 Å from the interface, and are partially strained through the remainder of the film.[8] The critical thickness has been observed between 200 and 1000 Å.[9] It is desirable to grow LSMO films with the benefits of strain, without the degradation resulting from relaxation.

Devices composed of LSMO and similar materials, such as those based on interlayer coupling and tunneling, require the ability to grow high quality multilayered heterostructures with sharp interfaces. This study is motivated by three goals: to exceed the limitations of critical thickness, to create new strain conditions, and to create structures with advanced functionality. Our approach is to use superlattices to introduce strain, not only at the substrate interface, but throughout the material. By selecting the interlayering material, the layer thickness, and the ratio between the two layers, we have additional degrees of freedom that can be controlled to optimize growth. The lattice mismatch at the substrate-film interface is by far the most significant source of strain in the system, but the strain introduced by the interlayering material can compensate some of the strain energy driving relaxation.

Superlattices of $La_{0.67}Sr_{0.33}MnO_3$ and $La_{0.67}Ca_{0.33}MnO_3$ indicate some of the difficulties faced in superlattice growth. Because both materials have a lattice parameter smaller than the STO substrate, more strain energy is created, driving the formation of defects. In the initial stages of growth, a layer–by–layer growth mode is indicated by reflection high-energy electron diffraction (RHEED) oscillations and atomic force microscopy (AFM) images show smooth surfaces with unit-

TABLE I. Summary of material properties.

	Unit Cell	Lattice parameter (Å)	Lattice mismatch with $SrTiO_3$ (%)	T_C (K)
$SrTiO_3$	Cubic	3.905	—	—
$La_{0.67}Sr_{0.33}MnO_3$	Rhombohedral	3.871	−0.82	340
$La_{0.67}Ba_{0.33}MnO_3$	Rhombohedral	3.91	+0.12	313

[a)]Author to whom correspondence should be addressed; electronic mail: eom@wisc.edu

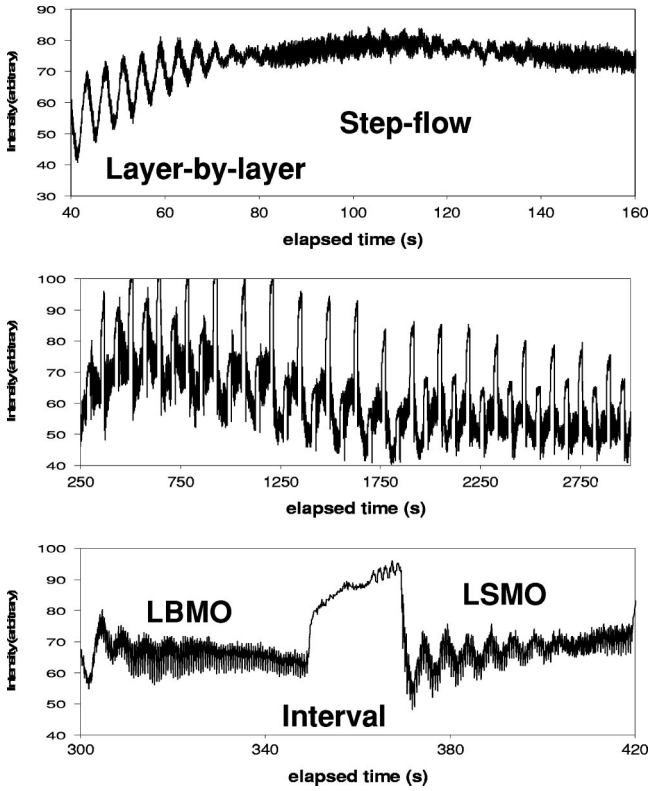

FIG. 1. Reflection high-energy electron diffraction (RHEED) intensity oscillations from (a) the growth of a single layer of LBMO, and (b) and (c) the growth of an LSMO-LBMO superlattice. In (a) the transition from layer–by–layer to step-flow growth mode is observed at about 80 s or 60 Å. (b) shows the regularity of the growth, sustained throughout the entire superlattice. In the expanded view (c), step-flow growth is observed in the LBMO layer (left), while in LSMO growth (right) oscillations are apparent.

cell high steps. After this first stage, the RHEED signal shows a marked decrease in intensity and oscillation amplitude until an abrupt recovery at approximately 200 Å. This recovery is believed to coincide with the formation of the defect-rich region and has been observed at about the same thickness in single layers of LSMO and LCMO. In AFM micrographs of these films none of the step or terrace features are seen due to the surface relaxation and defect structure.

Superlattices of LSMO and $La_{0.67}Ba_{0.33}MnO_3$ (LBMO) are of particular interest because of the chemical and structural compatibility of the two materials; summarized in Table I. Because of the difference in Curie temperature, there is a regime slightly above room temperature where the LSMO is ferromagnetic and the LBMO is paramagnetic. This is analogous to metallic giant magnetoresistance (GMR) devices. The lattice mismatch between LSMO and LBMO is 1.0%. More importantly, LSMO on STO grows in tension, whereas LBMO has a slightly larger lattice parameter and grows well in compression.[8] To a first approximation, assuming volume preservation of the unit cell and neglecting bulk modulus, this creates a compensating stress in the superlattice which decreases the driving force for relaxation.

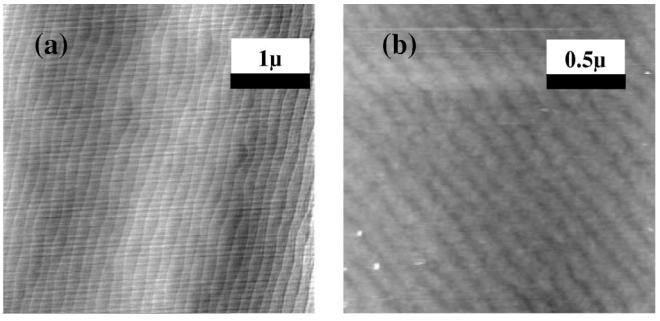

FIG. 2. Atomic force micrographs of (a) the surface of a single layer (200 Å) of LBMO on STO and (b) LSMO/LBMO superlattice. The step edges of the underlying, miscut substrate are visible and spaced about 120 Å apart, indicating a miscut angle of 0.2 Å. Section analysis shows single unit-cell steps.

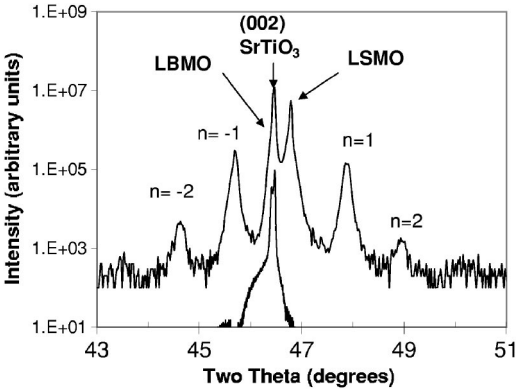

FIG. 3. X-ray diffraction $\theta-2\theta$ scan of LSMO-LBMO 128-layer superlattice (top) and LBMO single layer (bottom). Three sets of superlattice satellite peaks are visible.

We have grown a LBMO single layer and LSMO/LBMO superlattices by pulsed laser deposition with high-pressure *in situ* RHEED[10] on 0.2° miscut (001) $SrTiO_3$ substrates. These substrates were treated with buffered HF and annealed for TiO_2 surface termination. Depositions were performed at 780 °C, in 120 mTorr oxygen with an energy density of 2.2 J/cm^2 and a laser repetition rate of 5 Hz.[11] The LBMO film is approximately 200 Å thick. The superlattice layers were deposited with 200 laser pulses, corresponding to 11 unit cells, at a deposition rate, as indicated by RHEED intensity oscillations of about 18.2 pulses per atomic layer. This structure, 11 unit cells of each material, was repeated 64 times.

The initial growth of LBMO, as shown in Fig. 1(a), is characterized by distinct RHEED oscillations, indicating a layer–by–layer growth mode, which is the normal mode for LSMO films.[12] After approximately 60 Å, the oscillations disappear as the intensity recovery after each pulse becomes very rapid. This indicates very high adatom mobility on the surface and is associated with step-flow growth.[13] AFM images taken after the initial LBMO layer show straight steps edges without particles as in Fig. 2(a). The rms surface roughness is 4.7 Å. Although the section analysis shows some steps higher than one unit cell, the linear spacing of the step edges is the same for the final surface as for the substrate, therefore the additional height of the step edges is an artifact of the scan.

The RHEED trace of the superlattice [Fig. 1(b)] shows a uniform pattern for the two materials repeated over the duration of the deposition, approximately two hours. The inten-

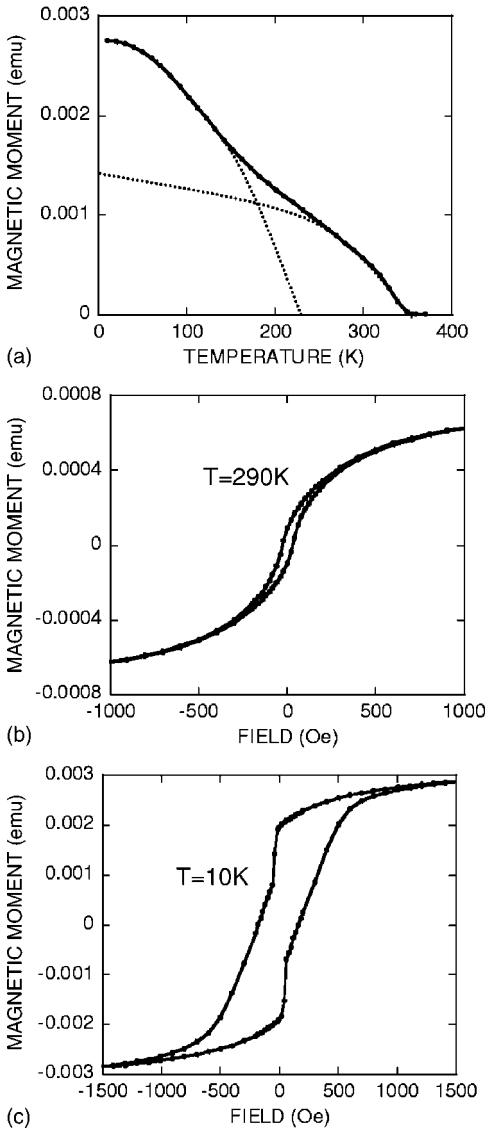

FIG. 4. Magnetization vs temperature of LSMO/LBMO superlattice (a) showing high T_c (~340 K) for LSMO and distinct T_C of LBMO around 250 K. Magnetization vs applied magnetic field for LSMO/LBMO superlattice show ferromagnetic behavior at 290 K (b) and independent coercivities of the two materials at 10 K (c).

sity suppression and recovery believed to correspond to defect formation and relaxation in LSMO and LCMO films is not observed in the LSMO/LBMO superlattice. Figure 1(c) is an expanded view of one LBMO/LSMO unit from Fig. 1(b). LBMO continues to grown in step-flow mode while some oscillations are apparent during LSMO growth. There is a strong, rapid recovery during the pause after each layer, indicating surface reconstruction. The AFM image taken after eight superlattice repetitions ending with LSMO (not shown), shows the morphology of the underlying substrate and the step spacing is unchanged. A large number of small islands of unit-cell height are apparent, consistent with layer–by–layer growth. After 128 layers, the step edges are still visible [Fig. 2(b)], however large; nonepitaxial boulders become a significant problem. The step spacing is consistent with that of the substrate surface, indicating that the steps are not bunched.

The x-ray diffraction θ–2θ scan shown in Fig. 3 shows the 002 reflection of the LSMO/LBMO superlattice along with a single layer (200 Å) LBMO. The out–of–plane lattice parameter of the single-layer LBMO is 3.91 Å; equal to the bulk value. The primary superlattice peak shows an out–of–plane lattice parameter of 3.87 Å, close to that of LSMO. Six superlattice peaks are seen, indicating a superlattice repetition unit of 90 ± 2 Å which is consistent with the thickness calculated from RHEED oscillations. Least-squares fits from the 002, 011, 111, 012, 021, 112, and 121 reflections show that the superlattice is strained to accommodate the substrate. The in-plane lattice parameters are 3.905 ± 0.003 Å and the out–of–plane lattice parameter is 3.872 ± 0.007 Å. The full width at half maximum of the rocking curve of the 002 peak is 0.02°.

The LSMO/LBMO superlattice was measured with a superconducting quantum interference device magnetometer as a function of temperature and applied field.[14] Figure 4(a) shows the M vs T curve, indicating two transitions. The T_C of LSMO is around 350 K, close to the bulk value. The T_C of LBMO is near 250 K which is significantly lower than the bulk value. Figure 4(b) shows the ferromagnetic hysteresis loop at 290 K, indicating only one transition. At 10 K, two coercivities are observed corresponding to independent switching of the LSMO and LBMO layers as seen in Fig. 4(c). The ferromagnetism at room temperature and the difference in the Curie temperatures is an important prerequisite to the fabrication of an all-oxide GMR structure.

We have fabricated superlattices of LSMO and LBMO by pulsed laser deposition. The RHEED, AFM, and x-ray diffraction confirm epitaxial growth. There is no evidence of the relaxation and defect formation seen in similar LSMO/LCMO superlattices.

The authors acknowledge the financial support of the NSF through Grant No. ECS-0210449.

[1] J. Z. Sun, Philos. Trans. R. Soc. London, Ser. A **356**(1742), 1693 (1998).
[2] S. C. Tidrow, A. Tauber, W. D. Wilber *et al.*, IEEE Trans. Appl. Supercond. **7**(2), 1766 (1997).
[3] M. Kawasaki, K. Takahashi, T. Maeda *et al.*, Science **266**, 1540 (1994).
[4] R. A. Rao, and C. B. Eom, Appl. Phys. Lett. **71**(9), 1171 (1997).
[5] R. A. Rao, D. Lavric, T. K. Nath *et al.*, Appl. Phys. Lett. **73**(22), 3294 (1998).
[6] F. Tsui, M. C. Smoak, T. K. Nath *et al.*, Appl. Phys. Lett. **76**(17), 2421 (2000).
[7] Y. Suzuki, H. Y. Hwang, S. W. Cheong *et al.*, Appl. Phys. Lett. **71**(1), 140 (1997).
[8] B. Wiedenhorst, C. Hofener, Y. F. Lu *et al.*, Appl. Phys. Lett. **74**(24), 3636 (1999).
[9] E. Favre-Nicolin and L. Ranno, J. Magn. Magn. Mater. **272–276**, (Part 3), 1814 (2004).
[10] G. Rijnders, G. Koster, D. H. A. Blank *et al.*, Appl. Phys. Lett. **70**(14), 1888 (1997).
[11] X. Ke, M. S. Rzchowski, L. J. Belenky *et al.*, Appl. Phys. Lett. **84**(26), 5458 (2004).
[12] M. Izumi, Y. Konishi, T. Nishihara *et al.*, Appl. Phys. Lett. **73**(17), 2497 (1998).
[13] J. Choi, C. B. Eom, G. Rijnders *et al.*, Appl. Phys. Lett. **79**(10), 1447 (2001).
[14] M. Sirena, N. Haberkorn, L. B. Steren *et al.*, J. Appl. Phys. **93**(10), 6177 (2003).